

01 Jan 1974

Performance Comparison Of Techniques For Obtaining Stereo Radar Images

George L. Bair

Gordon E. Carlson

Missouri University of Science and Technology

Follow this and additional works at: https://scholarsmine.mst.edu/ele_comeng_facwork



Part of the [Electrical and Computer Engineering Commons](#)

Recommended Citation

G. L. Bair and G. E. Carlson, "Performance Comparison Of Techniques For Obtaining Stereo Radar Images," *IEEE Transactions on Geoscience Electronics*, vol. 12, no. 4, pp. 114 - 122, Institute of Electrical and Electronics Engineers, Jan 1974.

The definitive version is available at <https://doi.org/10.1109/TGE.1974.294356>

This Article - Journal is brought to you for free and open access by Scholars' Mine. It has been accepted for inclusion in Electrical and Computer Engineering Faculty Research & Creative Works by an authorized administrator of Scholars' Mine. This work is protected by U. S. Copyright Law. Unauthorized use including reproduction for redistribution requires the permission of the copyright holder. For more information, please contact scholarsmine@mst.edu.

George L. Bair and Gordon E. Carlson
 University of Missouri-Rolla
 Rolla, Missouri

Abstract: The performance of three stereo radar techniques is compared with respect to both theoretical performance and performance in the presence of errors. The three techniques are: an improved single flight technique, a previously proposed single flight technique, and a two flight technique. Theoretical data for comparison of image parameters affecting performance have been generated with computer simulations of the imaging geometries for the techniques. The comparison shows that the improved technique will have images with greater similarity resulting in improved stereoviewability and measurability. Computer simulations have also been used to generate sensitivities of computed terrain point coordinates to system errors. These sensitivities are shown and overall error comparisons are made for assumed error values. These comparisons show that the improved single flight technique has the best error performance of the three techniques for the assumed reasonable set of system errors. This technique is followed by the previously proposed single flight technique and then the two flight technique.

Introduction

An improved single flight technique for obtaining stereo radar image pairs has been previously defined and the general advantages of this technique with respect to an implemented two flight technique and a previously proposed single flight technique have been discussed.¹ These advantages are that the two radar images are obtained with illumination from very nearly the same aircraft position which results in radar shadow and backscatter characteristics which are very similar and in improved image registration possibilities. These advantages enhance the photointerpretability and the stereoviewability of the stereo radar images.

The improved single flight technique uses a forward looking vertical fan radar beam pattern at an azimuth angle θ_F and a conical radar beam pattern with cone angle ϕ which lies in approximately the same direction as the fan beam pattern as shown in Fig. 1. This gives illumination angles which are nearly the same for the images generated with each radar beam pattern. However, the image displacement for elevated or depressed terrain points is the same for the conical radar beam pattern as for a side looking vertical fan radar beam pattern. This provides sufficient image displacement difference (parallax) between the two images so terrain height measurements can be made by viewing the image pair with a stereocomparator.

The previously proposed single flight technique uses two vertical fan radar beam patterns at different azimuth angles on the same aircraft as shown in plan view in Fig. 2. The illumination angle difference for the two images obtained is θ_0 and will thus be large. The previously implemented two flight technique uses a single side looking vertical fan radar beam pattern. The pair of stereo radar images are obtained on two flights at different elevation angles with respect to the terrain of interest as shown in elevation view in Fig. 3. This provides different image displacements for elevated or depressed terrain points on the two images but the images also will have a large illumination angle difference. Further details on the radar

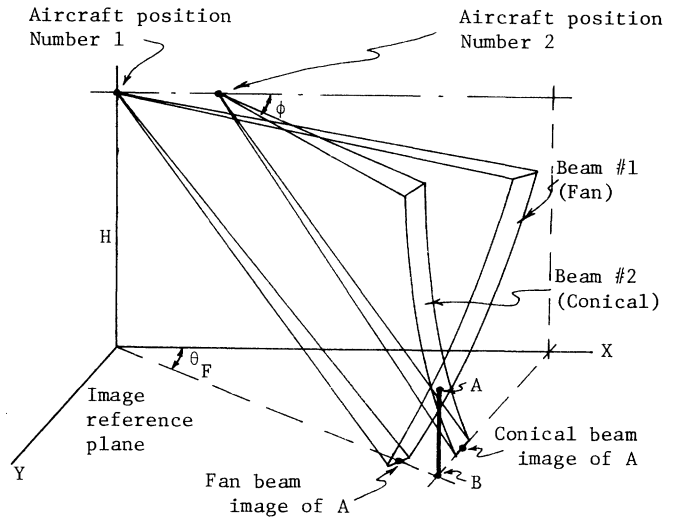


Fig. 1. Radar Beam Geometry for the Improved Single Flight Technique

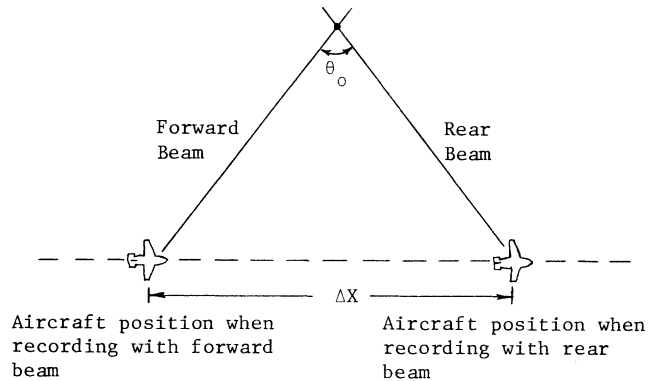


Fig. 2. Recording Flight Geometry for the Previous Single Flight Technique

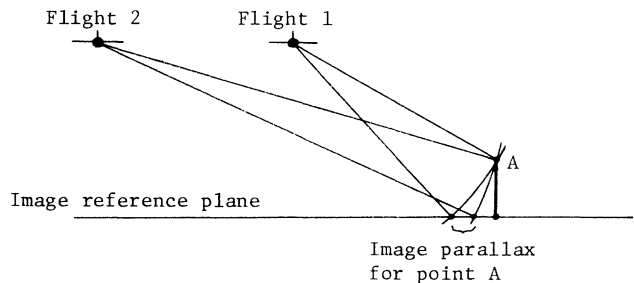


Fig. 3. Recording Flight Geometry for the Two Flight Technique

Manuscript received Feb. 7, 1974; revised June 27, 1974.

beam patterns and image characteristics mentioned above can be found in Ref. 1.

It is of interest to compare the performance of the three techniques in terms of both theoretical image characteristics and sensitivities to system errors. This paper presents the results of a quantitative determination of the values of image parameters which affect the relative advantages of the techniques. Also, the results of an error analysis for each of the techniques is shown in terms of sensitivities of computed terrain point coordinates to system errors. Error values are assumed and comparisons of the three techniques are made on the basis of the resulting errors in the computer terrain point coordinates for each technique.

System Parameters

System parameters for the three techniques must be chosen so they are comparable. It is of prime interest here how the improved single flight technique compares with the two previous techniques. Consequently, a desirable set of parameters for the improved single flight technique as established by a complete trade-off analysis⁶ is used. Parameters for the two previous techniques are chosen to make the parallax obtained approximately the same for all three techniques so they are comparable.

Trade-off analyses for the improved single flight technique have been performed with respect to: the vertical fan beam azimuth angle, the look down angle limits for the terrain swath being illuminated, the terrain swath width being imaged, and practical antenna lengths. The performance factors affected by these parameters are: the ratio of image parallax to terrain point height (parallax sensitivity) and the resolution which both affect the terrain height measuring capability, the illumination angle difference for the two images, the shadow length difference for the two images, the aircraft position separation when the two images are obtained, and the resolution difference between the two images. A computer simulation of the geometry of the system was used to examine a wide range of parameter values and arrive at a desirable set of parameters to be used for the improved single flight technique. The resulting radar and nominal operational parameters are shown in Table I for three different aircraft altitudes. The optimum pulsewidth, antenna length, and transmitter peak power all increase with aircraft altitude to give the values shown.

The radar transmission frequency has been chosen as large as practical considering atmospheric constraints (35 GHz) to limit the length of the array antennas required. The particular array lengths chosen give the best resolution and still keep the terrain being imaged in the far field. The pulsewidths were chosen to give compatible range and azimuth resolution. A nominal value of swath width is shown. Actually, the minimum grazing angle shown permits image swath widths which are four times as large as the nominal value; however, the parameters have been optimized for the nominal swath width and the wider swath widths are obtained only with degraded performance for that portion of the image swath beyond the nominal swath. Since azimuth resolution and range resolution are not constant across the image swath, an average value is shown. The height measuring accuracy value varies directly with the image azimuth resolution and inversely with the parallax sensitivity. Since both of these parameters vary across the image swath, an average value for height measuring accuracy is shown. This value was obtained by assuming that the parallax must be 50% of the image resolution before a terrain height differential can be measured. This is a reasonable

Table I. System Parameters for the Improved Single Flight Technique

Nominal Operational Parameters				
Aircraft Altitude (ft)	Swath Width (mi)	Avg. Az. Resolution (ft)	Avg. Range Resolution (ft)	Avg. Height Accuracy (ft)
3000	0.4	14	17	24
7500	1	22	27	38
15000	2	33	41	57
Radar Parameters				
Frequency	35 GHz			
Pulsewidth	0.025, 0.04, 0.06 μ sec			
PFR (Alternate Beam Transmission)	6000 pps			
Antenna	Fan Beam	Conical Beam		
Length	9.5, 15, 20 ft.	9.9, 15.6, 20.9 ft.		
Min. Grazing Angle	14.7°	15.1°		
Max. Grazing Angle	50.8°	50.0°		
Azimuth Angle	70.0°			
Cone Angle		75.06°		
Transmitter Peak Power	18,50,100 Kw			

assumption for radar images with the degree of similarity which will be attained with the improved single flight technique.

Theoretical Performance Comparison

The theoretical performance of the three techniques for obtaining stereo radar image pairs is compared in this section. In particular, the differences between the two images of the stereo pair are compared for the three techniques since these differences show the magnitude of the advantages previously mentioned. Table II shows these comparisons as well as the system parameters used to obtain the data. The data was obtained with computer simulations of the three techniques and is shown as a range of values which are the variation from the edge of the image swath nearest the aircraft to the edge of the image swath farthest from the aircraft. The improved single flight technique is chosen as the comparison base.

First, consider the comparison of the improved single flight technique with the previously proposed single flight technique. To make this comparison, it is assumed that the previously proposed single flight technique shown in Fig. 2 is implemented with its forward looking vertical fan radar beam pattern at the same azimuth angle as the forward looking vertical fan radar beam pattern for the improved single flight technique. It's rear looking vertical fan radar beam pattern is modified to be perpendicular to the flight path. This results in images with the same displacement geometries for the two techniques since the image displacements are the same for a side looking vertical fan radar beam pattern and a conical radar beam pattern with cone axis along the flight path. Therefore, the parallax sensitivities are the same, as is shown in Table II.

It can be seen, from Table II, that the aircraft position difference for the improved technique is 20%

Table II. Theoretical Performance Comparison of Three Stereo Radar Techniques

	Improved Technique	Previous Technique	Two Flight Technique
System Parameters			
Image Width (mi)	2	2	2.5
Aircraft Altitude (ft)	15,000	15,000	30,000
Beam #1			
Elevation Angle (deg)	50.8 to 32.6	50.8 to 32.6	38.0 to 30.2
Azimuth Angle (deg)	70	70	90
Beam #2			
Elevation Angle (deg)	50.0 to 32.9	52.6 to 34.2	50.0 to 38.0
Azimuth Angle (deg)	66.4 to 72.1	90	90
Cone Angle (deg)	75.06		
Image Parameters			
Parallax Sensitivity	0.445 to 0.232	0.445 to 0.232	0.410 to 0.200
Aircraft Position Difference (ft)	-849 to 918	4180 to 8040	13,200
Illumination Angle Difference (deg)	-3.71 to 2.13	15 to 17	12 to 7.8
Shadow Length Difference (Z)	2.58 to -1.28	6.8 to 6.5	52.5 to 34.4
Resolution Difference (Z)	-2.71 to 0.82	0	24.4 to 22.5

or less than that for the previous technique. For an aircraft velocity of 300 knots (506 ft/sec), the maximum time interval between the generation of the two images is 1.82 seconds for the improved technique and 15.9 seconds for the previous technique. The illumination angle difference for the improved technique is 25% or less than that for the previous technique and the shadow length difference is 38% or less. Actually, 85% of the swath width for the improved technique has an illumination angle difference which is less than 2.13° which means that the illumination difference over 85% of the swath width for the improved technique is 14% or less than that for the previous technique. The azimuth resolution difference for the previous technique is zero since the array lengths used to generate the two fan beams can be chosen to give equal azimuth resolution across both images. This can only be done for a single across flight path distance for the improved single flight technique images.

The height measuring accuracy for the two techniques is theoretically the same since the parallax is the same and the resolution can be made the same. However, the significantly greater distance between the aircraft positions when the two images are obtained for the previous technique makes relative aircraft position measurements less accurate which will make it more difficult to maintain relative image registration and accuracy and thus will degrade the height measuring performance. This is covered in more detail in the following error analysis section. Also, the image

differences indicated above will affect the stereo-viewability of the images which will impact the height measuring capability. This is a somewhat subjective effect and cannot be explored without the use of comparable radar imagery or simulated radar imagery.

The second theoretical performance comparison to be made is the comparison of the improved single flight technique with the presently implemented two flight technique. In this case, the two flight technique is not specified to have the same system parameters as the improved single flight technique. Instead, a set of parameters which has been utilized to obtain stereo radar imagery and which gives a swath of approximately the same width as the improved technique is considered so a comparison can be made with an existing imaging system. The images are obtained with a side looking radar on two flights past the image area as shown in Fig. 3. Actually, the illuminated swath on the ground is twice as wide as desired and the flights are flown with a 50% overlap. Therefore, the aircraft altitude is twice as large as for the improved technique to give approximately the same grazing angles and parallax sensitivity as the improved technique. Note that the image parameters also apply for a 2 mile wide image swath if the aircraft altitude is reduced by the same factor as the image swath width.

The parallax sensitivity for the improved technique is approximately 10% greater than for the two flight technique. Therefore, if the resolution is the same value for the two techniques, then the height measuring accuracy for the improved technique will be approximately 10% better than for the two flight technique. However, a synthetic array³ can be used to produce the images for the two flight technique and thus better resolution can be obtained with a resulting better theoretical height measuring capability.

The use of two flights means that it will be much more difficult to accurately establish the relative aircraft positions for the two images which will degrade the height measuring performance. This is a greater problem for the two flight technique than it was for the previously proposed single flight technique. Note that the aircraft position difference shown for the two flight technique is not really a comparable quantity with the single flight techniques since the distance is between two separate flight paths and not along a single flight path. The actual flight distance between illuminations, which is the important quantity from an accuracy standpoint, will depend on the length of the swath being mapped which determines the time interval between the two illuminations.

The illumination angle difference for the two flight technique is in the elevation angle direction and is approximately three times or more greater than for the improved technique. Shadow length differences are more than an order of magnitude larger for the two flight technique. This will produce a marked decrease in the number of terrain points which appear on both images and in image similarity. The resolution difference shown indicates that the two flight technique gives performance which is nearly an order of magnitude or more poorer than the improved technique; however, this is for a physical array antenna. If a synthetic array is used for the two flight technique, then it can be focused as a function of range which means that the azimuth resolution would be constant over the image and the azimuth resolution difference would be zero.

This theoretical performance comparison shows

that the improved single flight technique gives improved performance with respect to the previous single flight technique in all image difference parameters except resolution difference. The result will be an improved image pair with greater similarity and thus improved stereoviewability and measurability. The pair of images for the improved single flight technique are also much more similar than for the two flight technique which will enhance photointerpretability and stereoviewability which, in turn, will enhance terrain height measuring capabilities. However, a lower aircraft altitude, with respect to the two flight technique, is required to obtain the necessary resolution with the physical array antennas required for the single flight techniques. This results in a shorter stand-off distance from the aircraft flight path to the terrain swath being imaged.

Error Performance Comparison

The performance of the three stereo radar techniques in the presence of system errors is required in order to be able to compare them more completely. This performance comparison is obtained in terms of the sensitivities of the computed terrain point coordinates (X_R = along flight path orthographic position, Y_R = across flight path orthographic position, and h_R = height) to the various system errors and in terms of the standard deviations and correlations of the computed terrain point coordinate errors which result from assumed practical values of system errors. The individual error sources considered in analyzing the error performance are: radar ranging (ΔR), aircraft altitude (ΔH), along flight path aircraft position (ΔX_A), across flight path aircraft position (ΔY_A), along flight path image recording position (ΔX_I), across flight path image recording position (ΔY_I), antenna roll angle ($\Delta \alpha$), antenna pitch angle ($\Delta \beta$), antenna yaw angle ($\Delta \gamma$), and conical beam cone angle ($\Delta \phi$). Note that the antennas are assumed to be space stabilized so that the angular errors to be considered are antenna stabilization errors with respect to the desired level flight path as indicated above. The order in which the angular errors are taken is yaw, pitch, roll.

The system errors are assumed to be short-term independent errors for initial analysis purposes. This is done since the correlations in an actual system will be mechanization dependent and it is felt that independent error sources provide a reasonable assumption for error performance comparison. Additional discussion supporting the validity of this assumption and indicating the effect of some known highly correlated errors is presented after the overall system error sensitivities have been presented.

For this investigation, all angular errors are assumed to have short-term standard deviations of 0.01 degree which appears to be within the state-of-the-art for the antenna stabilization. All aircraft position errors are assumed to have short-term standard deviations of 1 foot. This is an attainable short-term navigation error for a high quality inertial navigation system. Ranging and imaging errors are assumed to have a standard deviation of 1 foot, 2.5 feet, or 5 feet for aircraft altitudes of 3,000 feet, 7,500 feet, or 15,000 feet, respectively. This corresponds to approximately 0.1% accuracy with respect to one-half of a nominal swath width.

Error Analysis Method

A computer simulation was used to perform the error analyses required for the error performance comparison. Equations relating image positions to system parameters and errors and equations needed to compute the terrain point coordinates from the measured image

position data are required for this simulation and error analysis. They are discussed after the error analysis method is outlined.

The equations which relate input system parameters and errors to output terrain point coordinates are complex and nonlinear. Monte Carlo techniques were considered to perform the error analysis for the complex total system; however, much computation would have been required to evaluate the results across the swath for a range of terrain heights. Therefore, it was felt that this approach was not justified. This is especially true since the assumed errors are small which means that good error results are attainable by computing terrain point coordinate error sensitivities to individual error sources and using these sensitivities in a linearized error analysis to transform the covariance matrix of the input system errors into the covariance matrix of the computed terrain point errors.⁴ Two additional reasons which make this method a desirable choice are: (1) the sensitivities are desired to determine which errors limit the error performance and, (2) the complex equations required for the computation of the image positions are considerably simplified if only one system angular error needs to be considered at a time. This is particularly true for the conical beam image.

Sensitivities were computed for each error source for a range of terrain point across flight path positions and heights. The individual error sensitivities were determined by computing the difference between the computed terrain point coordinates obtained for a small error magnitude and the actual terrain point coordinates and dividing this difference by the error value. Reasonable variations in terrain point height do not greatly effect the error sensitivities; therefore, they are neglected. Some of the sensitivities are dependent upon terrain point across flight path position. Therefore, the average sensitivities are used to present results and make comparisons.

Image Position Coordinate Equations

Equations relating the image position coordinates to system parameters and errors for images generated by vertical fan and conical radar beams have been developed.² The development is quite lengthy and is not included here; however, the resulting equations are shown below. The individual error sources considered in formulating these equations are those previously mentioned. Other parameters required in the equations presented below are: terrain point across flight path position (Y), terrain point altitude (h), aircraft altitude (H), vertical fan beam look angle (θ_F), and conical beam cone angle (ϕ). The coordinate frame for which the equations are derived has its X axis along the flight path ground track and its Y axis perpendicular to the flight path ground track and passing through the projection of the terrain point on the reference plane.

The equations which express the image coordinates X_F and Y_F for the fan beam image are:

$$X_F = X_{AF} + R_{GF} \cos \theta_F + \Delta X_I - \Delta X_A$$

$$Y_F = R_{GF} \sin \theta_F + \Delta Y_I$$

where

$$X_{AF} = \frac{Y_E (B_{X^*P} - B_{Z^*P}) + H_D (B_{Y^*P} - B_{X^*Y})}{A}$$

$$R_{GF} = [([r^2 + s^2]^{1/2} + \Delta R)^2 - H^2]^{1/2}$$

$$H_D = H_E - h, \phi_1 = \phi + \Delta\phi$$

and

$$B = \cos^2 \Delta\gamma - \cos^2 \phi_1, C = \cos^2 \Delta\beta - \cos^2 \phi_1$$

$$Y_E = Y - \Delta Y_A, H_E = H + \Delta H, H_D = H_E - h$$

$$r = \frac{B_Z Y_E - B_Y H_D}{A}, s = \frac{P_Y H_D - P_Z Y_E}{A}$$

$$P_X = \sin \Delta\beta, P_Y = -\sin \Delta\alpha, P_Z = \cos \Delta\alpha \cos \Delta\beta$$

$$B_X = \cos \theta_F \cos \Delta\beta \cos \Delta\gamma - \sin \Delta\gamma \sin \theta_F$$

$$B_Y = \cos \theta_F \sin \Delta\gamma + \sin \theta_F \cos \Delta\alpha \cos \Delta\gamma$$

$$B_Z = -\cos \theta_F \sin \Delta\beta + \sin \theta_F \sin \Delta\alpha$$

$$A = B_Z P_Y - B_Y P_Z$$

The equations which express the image coordinates X_C and Y_C for the conical beam image are:

$$X_C = X_{AC} + R_C \cos \phi + \Delta X_I - \Delta X_A$$

$$Y_C = R_{GC} + \Delta Y_I$$

where

$$X_{AC} = \frac{Y_E \sin \Delta\gamma \cos \Delta\gamma - \cos \phi_1 [Y_E^2 \sin^2 \phi_1 + H_D^2 B]^{1/2}}{B}$$

for any error except a pitch angle error, and

$$X_{AC} = \frac{-H_D \sin \Delta\beta \cos \Delta\beta - \cos \phi_1 [Y_E^2 C + H_D^2 \sin^2 \phi_1]^{1/2}}{C}$$

for a pitch angle error. In addition,

$$R_C = [X_{AC}^2 + Y_E^2 + H_D^2]^{1/2} + \Delta R$$

$$R_{GC} = [R_C^2 \sin^2 \phi - H^2]^{1/2}$$

and

$$Y_E = Y - \Delta Y_A, H_E = H + \Delta H$$

The equations shown above are sufficient to analyze all three stereo radar techniques since each technique has vertical fan or conical radar beam patterns. It should be emphasized that the trigonometric expressions in these equations have been simplified so they are valid only if not more than one angular error is evaluated at one time.

Terrain Point Coordinate Equations

Since comparison of the error performance of the three techniques is made on the basis of the computed terrain point coordinates, the equations to be used to compute the terrain point coordinates from the measured image positions on the pair of stereo images must be known for each technique. There are only three terrain point coordinates (X_R, Y_R, h_R) to be computed with four image measurement values (X and Y coordinates measured on each image). This indicates that there could be four equations for each terrain point coordinate with each equation in terms of three of the image position coordinates.

The image positions for the improved single flight technique as well as the orthographic position of the terrain point corresponding to the images are shown in the superimposed stereo radar pair of images shown in Fig. 4 as an aid to discussing the required equations. The image coordinates for the forward looking vertical fan beam are (X_F, Y_F), the image coordinates for the conical beam are (X_C, Y_C), and θ_F is the azimuth angle of the forward looking vertical fan beam. Actual image position measurements are made with a stereocomparator with the images oriented so the operator's eye base is perpendicular to the azimuth line defined by the forward looking fan beam azimuth angle to obtain maximum parallax and therefore maximum height measuring accuracy. The resulting

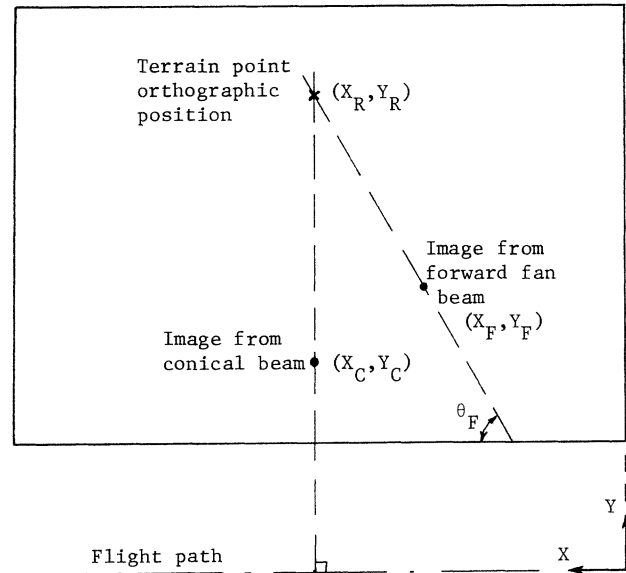


Fig. 4. Superimposed Improved Single Flight Stereo Radar Images

measurements are converted into equivalent measurements in the X, Y (along flight path, across flight path) coordinate frame of reference shown in Fig. 4.

For the improved single flight technique, there are only two equations for X_R , three equations for Y_R , and three equations for h_R since two of the image position coordinates do not depend on X_R and one image position coordinate does not depend on either Y_R or h_R . These equations are:

$$X_{R1} = X_C$$

$$Y_{R1} = Y_F + (X_C - X_F) \tan \theta_F$$

$$h_{R1} = H - [H^2 - (Y_{R1}^2 - Y_F^2) \csc^2 \theta_F]^{1/2}$$

$$X_{R2} = X_F - Y_F \cot \theta_F + \csc \theta_F [Y_F^2 - Y_C^2 \sin^2 \theta_F]^{1/2}$$

$$Y_{R2} = \sec \theta_F [Y_F^2 - Y_C^2 \sin^2 \theta_F]^{1/2}$$

$$h_{R2} = H - [H^2 - (Y_F^2 - Y_C^2) \sec^2 \theta_F]^{1/2}$$

$$Y_{R3} = \frac{2(X_C - X_F)}{\sin 2\theta_F} + [(X_F - X_C)^2 \csc^2 \theta_F + Y_C^2]^{1/2}$$

$$h_{R3} = H - [H^2 - Y_{R3}^2 + Y_C^2]^{1/2}$$

The covariance matrix for the solutions for each coordinate were computed using the system error magnitudes previously assumed, the system parameters defined in Table II, and the average error sensitivities. The standard deviations for the errors in the two solutions for X_R are: $\sigma_{XR1} = 7.66$ ft. and $\sigma_{XR2} = 28.6$ ft. The correlation coefficient for the two solution errors is $\rho_{XR1, XR2} = 0.03$. The standard deviations and correlation coefficients for the errors in the three solutions for Y_R are: $\sigma_{YR1} = 28.4$ ft., $\sigma_{YR2} = 80.7$ ft., $\sigma_{YR3} = 32.0$ ft., $\rho_{YR1, YR2} = 0.18$, $\rho_{YR1, YR3} = 0.95$, and $\rho_{YR2, YR3} = -0.15$. The standard deviations and correlation coefficients for the errors in the three solutions for h_R are: $\sigma_{hR1} = 35.4$ ft., $\sigma_{hR2} = 97.7$ ft., $\sigma_{hR3} = 35.4$ ft., $\rho_{hR1, hR2} = 0.08$, $\rho_{hR1, hR3} = 0.99$, and $\rho_{hR2, hR3} = 0.09$. It can be seen that one equation for X_R is considerably less sensitive to system errors. For Y_R and h_R , two equations are considerably less sensitive to system errors than the third. In addition, the two equations which are least sensitive to system errors also produce solution errors which are highly correlated.

A least squares weighting of the equations indicated was considered as a method for obtaining a least error sensitive set of equations relating the terrain point coordinates to the image position coordinates. However, the relative magnitude of the various solution errors due to system errors and the high degree of cor-

relation for the two best solutions for Y_R and h_R indicate that not much additional improvement is possible using the more complex least squares weighted equations to compute terrain point coordinates. An additional negative aspect is the fact that the weighting factors would actually be a function of the Y position of the terrain point being considered. Therefore, it was decided that simply using the set of equations which is least sensitive to system errors made the most sense from a practical point of view. Actually, the solutions X_{R1} , Y_{R1} and h_{R3} were chosen since they were the simplest and h_{R3} gives the same performance as h_{R1} . This choice also gives a slight improvement in the error sensitivity for the computation of the terrain height h_R which results in a standard deviation of 34.2 ft. for the h_R solution error with the assumed system error magnitudes. The decision to use the set of equations which is least sensitive to system errors was checked by obtaining the least squares weighted terrain point coordinate equations and evaluating the resulting computed terrain point coordinate errors using the same conditions and parameters as above. The decrease in the standard deviations of the computed coordinate errors using these much more complex equations is 0.2 ft. for X_R , 0.4 ft. for Y_R and 0.1 ft. for h_R which shows that the greater complexity is not warranted and therefore the terrain point coordinate equations chosen are a good choice.

The image displacement geometry for the previously proposed single flight technique is the same as for the improved single flight technique which was shown in Fig. 4. Thus, the terrain point coordinate equations possible for the previously proposed single flight technique are identical to those for the improved single flight technique. The same set of equations was chosen for this technique as for the improved single flight technique. The similarity of error sensitivities to those for the improved single flight technique indicates that this is a reasonable choice.

The image positions for the two flight technique, as well as the orthographic position of the terrain point corresponding to the images are shown in the superimposed stereo pair of images shown in Fig. 5. In this case, image position measurements are made with

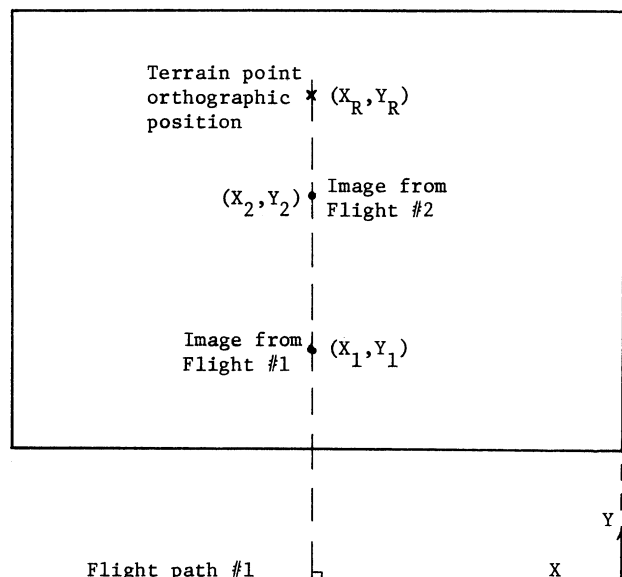


Fig. 5. Superimposed Two Flight Stereo Radar Images

the operator's eye base perpendicular to the flight path direction.

The equations for computing the terrain point coordinates Y_R and h_R for the two flight technique are unique so no selection is necessary. There are two solutions possible for the X_R terrain point coordinate which are the along flight path positions on each flight. The X_R coordinate is obtained by averaging the two possible solutions. This is not the optimum weighting in the least squares sense since the variances of the two solutions are not equal and the difference in variance changes across the image. However, the variances are sufficiently close in magnitude to recommend this simple formulation. The set of equations for computing the terrain point coordinates is then

$$X_R = 0.5(X_1 + X_2)$$

$$Y_R = \frac{Y_2^2 - Y_1^2 + 2Y_2 S}{2S}$$

$$h_R = H - [H^2 + Y_1^2 - Y_R^2]^{\frac{1}{2}}$$

where: (X_1, Y_1) are the image position coordinates for Flight #1, (X_2, Y_2) are the image position coordinates for Flight #2 and S is the flight path separation distance for the two flights.

Error Performance Results

The error analysis method, equations, and error magnitudes presented have been applied to each of the three stereo radar techniques for several terrain points across the image swath. As has been indicated, some of these sensitivities depend on the across flight path position (Y) of the terrain point being considered. The greatest error sensitivity variability is in the error sensitivities for the height coordinate h_R . Many of these sensitivities vary by approximately a factor of two over the swath with the greatest variability being for the sensitivity of h_R to antenna yaw angle error which varies by a factor of approximately 3.5. The variations are nearly linear so the average sensitivities do give a good measure of average performance. The average sensitivities for the error sources considered are shown in Table III, IV and V for the same system parameters as were previously used for system comparison and which are shown in Table II. Note that separate sensitivities are shown for errors encountered in obtaining each image of the stereo pair. These tables are also applicable for other aircraft altitudes since position error sensitivities are unchanged and angular error sensitivities scale directly with altitude.

The limiting error sources with the assumed error magnitudes are different for the single flight techniques than for the two flight technique. In the case of the single flight techniques, the limiting error sources are the angular errors and image position errors while the limiting error sources for the two flight technique are the aircraft and image position errors. Actually the angular errors limit the X_R position accuracy for the two flight technique but its error is considerably smaller than for Y_R and h_R , so the position errors can be considered as the limiting errors.

Table III. Error Sensitivities of the Computed Terrain Point Coordinates for the Improved Single Flight Technique

Error ΔE	ΔX _R /ΔE	ΔY _R /ΔE	Δh _R /ΔE
Ranging (C)	0.25	0.68	-0.70
Ranging (F)	0	0	0
Image Y Pos. (C)	0	0	-1.13
Image Y Pos. (F)	0	1.00	1.13
Image X Pos. (C)	1.00	2.75	3.10
Image X Pos. (F)	0	-2.75	-3.10
A/C Alt. (C)	0	0	-1.00
A/C Alt. (F)	0	0	0
A/C Y Pos. (C)	0	0	1.13
A/C Y Pos. (F)	0	-1.00	-1.13
A/C X Pos. (C)	-1.00	-2.75	-3.10
A/C X Pos. (F)	0	2.75	3.10
A/C Roll (F)	0	261.75	294.6
A/C Pitch (C)	-261.78	-719.24	-910.23
A/C Pitch (F)	0	719.34	810.19
A/C Yaw (C)	294.55	809.27	1073.85
A/C Yaw (F)	0	-916.42	-1079.85
Cone Angle	396.33	1088.92	1436.50

Units: Distance Quantities - Ft/Ft
Angles - Ft/Deg

(C) = Conical Beam, (F) = Fan Beam

While the sensitivities shown are useful in establishing the relative effects of various error sources, the most useful error performance comparison is made when typical error values are assigned. Typical short-term independent error values were given earlier in this section. These assumed error magnitudes are satisfactory for the improved single flight technique. However, analysis of the three techniques has shown that the distance the aircraft travels between the two illuminations of a specific terrain point is different for each technique. For the improved single flight technique, this distance is less than 1,000 feet. For the previous single flight technique, this distance has a maximum value of approximately 10,000 feet. For the two flight technique, this distance is likely to be very large because of the necessity of making two flights past the terrain area of interest. For example, if a map fifteen miles long is being made, then the average distance flown between illuminations is about 100,000 feet.

Since the previous two techniques have significantly (orders of magnitude) greater time between illumination of the two images, the aircraft altitude and position errors and the slant ranging error will be longer term errors and will have a larger standard deviation than those used for the improved single flight technique. For comparison purposes, it is assumed that the standard deviation of these errors is twice as large for the previous single flight technique and three times as large for the two flight technique. Using these assumed errors, the covariance matrix of the computed terrain point coordinates were

Table IV. Error Sensitivities of the Computed Terrain Point Coordinates for the Previous Single Flight Technique

Error ΔE	$\Delta X_R/\Delta E$	$\Delta Y_R/\Delta E$	$\Delta h_R/\Delta E$
Ranging (2)	0	0	-1.51
Ranging (1)	0	0	0
Image Y Pos. (2)	0	0	-1.13
Image Y Pos. (1)	0	1.00	1.13
Image X Pos. (2)	1.00	2.75	3.10
Image X Pos. (1)	0	-2.75	-3.10
A/C Alt. (2)	0	0	-1.00
A/C Alt. (1)	0	0	0
A/C Y Pos. (2)	0	0	1.13
A/C Y Pos. (1)	0	-1.00	-1.13
A/C X Pos. (2)	-1.00	-2.75	-3.10
A/C X Pos. (1)	0	2.75	3.10
A/C Roll (1)	0	261.75	294.61
A/C Pitch (2)	-261.8	-719.29	-808.57
A/C Pitch (1)	0	719.34	810.19
A/C Yaw (2)	294.57	809.32	956.10
A/C Yaw (1)	0	-916.42	-1079.85

Units: Distance Quantities - Ft/Ft
Angles - Ft/Deg

(1) = Forward Fan Beam, (2) = Side Fan Beam

Table V. Error Sensitivities of the Computed Terrain Point Coordinates for the Two Flight Technique

Error ΔE	$\Delta X_R/\Delta E$	$\Delta Y_R/\Delta E$	$\Delta h_R/\Delta E$
Ranging (2)	0	-3.32	-5.01
Ranging (1)	0	4.10	4.39
Image Y Pos. (2)	0	-2.41	-3.67
Image Y Pos. (1)	0	3.41	3.67
Image X Pos. (2)	0.50	0	0
Image X Pos. (1)	0.50	0	0
A/C Alt. (2)	0	-2.27	-3.40
A/C Alt. (1)	0	2.27	2.41
A/C Y Pos. (2)	0	2.41	3.67
A/C Y Pos. (1)	0	-3.41	-3.67
A/C X Pos. (2)	-0.50	0	0
A/C X Pos. (1)	-0.50	0	0
A/C Pitch (2)	-261.80	-0.21	-0.26
A/C Pitch (1)	-261.80	0.21	0.22
A/C Yaw (2)	277.27	0.24	-0.37
A/C Yaw (1)	392.46	0.472	0.52

Units: Distance Quantities - Ft/Ft
Angles - Ft/Deg

(1) = Flight #1, (2) = Flight #2

computed for each stereo radar technique. The resulting standard deviations of the computed terrain point coordinates are error quantities of prime interest for performance comparison and are shown in Table VI. The data show that the improved single flight technique has the best error performance and that both single flight techniques perform better than the two flight technique. It should be noted that the error in measuring terrain altitude for the improved single flight technique is compatible with the theoretical height measuring accuracy shown in Table I. This indicates that the error magnitudes chosen are approximately the stabilization and position accuracies required for the improved single flight technique.

While the correlation of the computed terrain point coordinate errors is not highly significant from the standpoint of error performance comparison of the three techniques, it is of interest as an indicator of expected error configurations. The correlation matrix for the improved single flight technique is

$$\begin{bmatrix} 1 & 0.74 & 0.72 \\ 0.74 & 1 & 0.96 \\ 0.72 & 0.96 & 1 \end{bmatrix}$$

while the correlation matrix for the previously proposed single flight technique is

Table VI. Standard Deviations of the Computed Terrain Point Coordinates for the Three Stereo Techniques

Coordinate Error	Technique		
	Improved Single Flight	Previous Single Flight	Two Flight
σ_{X_R}	7.66 ft	9.55 ft	18.6 ft
σ_{Y_R}	28.4 ft	38.8 ft	83.3 ft
σ_{h_R}	34.2 ft	47.5 ft	105 ft

$$\begin{bmatrix} 1 & 0.68 & 0.63 \\ 0.68 & 1 & 0.94 \\ 0.63 & 0.94 & 1 \end{bmatrix}$$

and the correlation matrix for the two flight technique is

$$\begin{bmatrix} 1 & 7 \times 10^{-5} & 5 \times 10^{-5} \\ 7 \times 10^{-5} & 1 & 0.98 \\ 5 \times 10^{-5} & 0.98 & 1 \end{bmatrix}$$

where the order of the computed terrain point coordinates is taken to be X_R, Y_R, h_R . For all techniques, the computed across flight path coordinate error is highly correlated with the computed terrain height error. Considerable correlation of the along flight path coordinate error is also evidenced for the single flight techniques. However, the computed along flight path coordinate error for the two flight technique is basically uncorrelated with the other two errors. This is as expected since only X image coordinates are used to compute the along flight path coordinate and only Y image coordinates are used to compute the other two coordinates. The only coupling between these image positions occurs because of antenna angular errors to which the Y image coordinates are very insensitive.

The error sensitivities obtained above for the techniques can be used to support further comments with respect to the independent error assumption used for the error performance comparison and with respect to the effect of correlated errors. System errors which are highly correlated from one image to the other will have reduced effect due to cancellation in most cases as is indicated by the sensitivities shown. A notable exception to this cancellation is the case of aircraft position errors in which case highly correlated errors shift the two images as a unit. This causes systematic image shifts which would be removed in the final image processing by using control points. Consequently, the aircraft position errors which affect the performance comparison are those related to short-term random phenomena.

The sensitivities to antenna stabilization angular errors show that any direct correlation of the angular errors will improve the overall error performance; however, negative correlation of the yaw angle error with the other two errors will degrade performance. This information would be useful in considering the design of the antenna stabilization system. Independence of the remaining radar and image recording errors is a reasonable assumption for comparison purposes. In view of the above considerations, short-term independent random errors are a reasonable assumption for error performance comparison of the three techniques since in general they have the greatest impact of the final compensated error performance of the system.

A performance comparison of three stereo radar techniques has been shown. The theoretical performance parameters considered are those which affect the similarity of the two images in the stereo pair obtained. This similarity or lack of it will have considerable impact on the photointerpretability and stereoviewability of the resulting image pairs. The comparison of these parameters has shown that the improved single flight technique gives improved performance with respect to the previous single flight technique. The pair of images for the improved single flight technique is also much more similar than for the two flight technique. Thus, in both cases, terrain height measuring capability will be enhanced.

The error performance for the three techniques has been shown in terms of the sensitivities of the computed terrain point coordinates to system errors and in terms of the standard deviations and correlations of the error in the computed terrain point coordinates due to an assumed set of system error values. The sensitivities are valuable in showing the relative effect of various error sources and these relative effects are noted. The computed terrain point coordinate error comparison shows that the improved single flight technique has the best error performance of the three techniques for the assumed reasonable set of error source values.

Acknowledgment

This work was supported by the Geography Programs Branch of the Office of Naval Research under contract number N00014-69-A-0141-0008 and contract authority identification number NR387-069.

References

1. G. E. Carlson, "An Improved Single Flight Technique for Radar Stereo", IEEE Trans. on Geoscience Electronics, Vol. GE-11, No. 4, pp. 199-204, (October 1973).
2. G. E. Carlson and G. L. Bair, "Single Flight Radar Using a Mechanically Slew Array and an Electrically Squinted Array", University of Missouri-Rolla, Communications Sciences Report, CSR-73-5, (November 1973). (AD771434)
3. L. J. Cutrona, "Synthetic Aperture Radar", in M. I. Skolnik, Radar Handbook, New York: McGraw-Hill, (1970), ch. 23.
4. A. M. Breipohl, Probabilistic Systems Analysis, New York: John Wiley and Sons, Inc., (1970).